11 (2014) 437 - 458

Latin American Journal of Solids and Structures

www.lajss.org

Exact solution for thermo-mechanical vibration of orthotropic mono-layer graphene sheet embedded in an elastic medium

Abstract

In this paper, the effect of the temperature change on the vibration frequency of mono-layer graphene sheet embedded in an elastic medium are studied. Using the nonlocal elasticity theory, the governing equations are derived for single-layered graphene sheets. Using Levy and Navier solutions, analytical frequency equations for single-layered graphene sheets are obtained. Using Levy solution, the frequency equation and mode shapes of orthotropic rectangular nanoplate are considered for three cases of boundary conditions. The obtained results are subsequently compared with valid result reported in the literature. The effects of the small scale, temperature change, different boundary conditions, Winkler and Pasternak foundations, material properties and aspect ratios on natural frequencies are investigated. It has been shown that the non-dimensional frequency decreases with increasing temperature change. The present analysis results can be used for the design of the next generation of nanodevices that make use of the thermal vibration properties of the nanoplates.

Keywords

Thermo-mechanical vibration; Orthotropic single-layered graphene sheets; Elastic medium; Analytical modeling.

M. Mohammadi [a, b *]
A. Moradi [a]
M. Ghayour [b]
A. Farajpour [b]

[a] Department of engineering, Ahvaz branch, Islamic Azad University, Ahvaz, Iran.
[b] Department of mechanical engineering, Isfahan University of Technology, Isfahan 84156-83111, Iran.

Received in 24 Mar 2013
In revised form 12 Jun 2013

*Author email: m.mohamadi@me.iut.ac.ir

1 INTRODUCTION

Nano-materials have attracted attention of many researchers in this field due to their novel properties. Many scientific communities study the characteristics of nanomaterials such as carbon nanotubes (CNTs), nanoplates, nanorods and nanorings. To design plate efficiently, we need to understand their vibration behavior. Vibration of 'scale-free' plates has been studied widely in the literatures which this theory cannot predict the size effects. Thus, in with small size, long-range inter-atomic and inter-molecular, cohesive forces cannot be ignored because they strongly affect

the static and dynamic properties (Wong et al 1997; Sorop and Jongh 2007). To use graphene sheets properly as design nano electro-mechanical system and micro electro-mechanical systems (NEMS and MEMS) component, their frequency response with small-scale effects should be investigated.

Graphene is a truly two-dimensional atomic crystal with exceptional electronic and mechanical properties. Many nanostructures based on the carbon such as carbon nanotube (Iijima 1991), nanorings (Kong et al 2004), etc. are considered as deformed graphene sheet so analysis of graphene sheets is a basic matter in the study of the nanomaterials.

Continuum modeling of CNTs has also attracted and increasing deal of attention of many researchers due to experiments in nanoscale is difficult and molecular dynamic simulations are highly computationally expensive. There are various size-dependent continuum theories such as couple stress theory (Zhou and Li 2001), strain gradient elasticity theory (Fleck, and Hutchinson 1997; Akgöz and Civalek 2011a; Akgöz and Civalek 2012a; Akgöz and Civalek 2013a), modified couple stress theory (Yang et al 2002; Akgöz and Civalek 2011b; Akgöz and Civalek 2012b; Akgöz and Civalek 2013b) and nonlocal elasticity theory (Eringen 1983). Among these theories, nonlocal elasticity theory has been widely applied (Murmu and Pradhan, 2009; Babaei and Shahidi 2010; Moosavi et al 2011; Farajpour et al 2011a; Mohammadi et al 2013a; Civalek et al. 2010; Civalek and Demir 2011; Demir and Civalek 2013; Civalek and Akgöz 2013) that this theory was introduced by Eringen (1983). He modified the classical continuum mechanics to take into account small scale effects. In this theory, the stress state at a given point depends on the strain states at all points, while in the local theory, the stress state at any given point depends only on the strain state at that point. Murmu and Pradhan (2009) employed the nonlocal elasticity theory for the vibration analysis of rectangular single-layered graphene sheets embedded in an elastic medium. They have used Both Winkler-type and Pasternak-type models for simulate the interaction of the graphene sheets with a surrounding elastic medium. They reported that the natural frequencies of single-layered graphene sheets are strongly dependent on the small scale coefficients. Pradhan and Phadikar (2009) investigated the vibration of embedded multilayered graphene sheets (MLGS) based on nonlocal continuum models. In thier paper, they have shown that nonlocal effect is quite significant and needs to be included in the continuum model of graphene sheet. Wang et al. (2011) studied the vibration of double-layered nanoplate. In their research, it is concluded thermal effect and nanoplate with isotropic mechanical properties. It has been reported that graphene sheets have orthotropic properties (Reddy et al 2006). Malekzadeh et al. (2011) used the differential quadrature method (DQM) to study the thermal buckling of a quadrilateral nanoplates embedded in an elastic medium. Aksencer and Aydogdu (2011) proposed levy type solution for vibration and buckling of nanoplate. In that paper, they considered rectangular nanoplate with isotropic property and without effect of elastic medium. Thermal vibration analysis of orthotropic nanoplates based on nonlocal continuum mechanics were studied by Satish et al. (2012) who considerate two variable reinfined plate theory for thermal vibration of orthotropic nanoplate. In general, single layered graphene sheets are embedded in an elastic medium but they didn't consider effect of elastic medium in that paper. On the other hand, they represented vibration frequency of rectangular nanoplate only for simply supported boundary conditions and they didn't represent vibration frequency for other boundary conditions. Some researches of the nanoplates

have been reported on the mechanical properties. However, compared to the nanotubes, studies for the nanoplates are very limited, particularly for the mechanical properties with thermal effects.

In the present study, the effect of the temperature change on the vibration frequency of orthotropic monolayer graphene sheets embedded in an elastic medium is investigated. The governing equations of motion are derived using the nonlocal elasticity theory. Levy type solution for the vibration of orthotropic rectangular nanoplate under thermal effect and elastic medium is obtained. Unlike the case of an isotropic plate that the roots are easily seen repeated roots but for this case there are four sets because the roots depend on the relative stiffness of the nanoplate in various directions, effect of elastic medium and temperature change. Hence, in this study for the thermal vibration of orthotropic rectangular nanoplate in an elastic medium using the Levy-type solution requires four different forms for the homogeneous solution. The small scale effects and thermal effect on the vibrations frequency of graphene sheets with three set boundary conditions are investigated. The thermal effects, effect of boundary condition and some other impressions on the vibration properties are investigated. From the results, some new and absorbing phenomena can be observed. To suitably design nano electro-mechanical system and micro electro-mechanical systems (NEMS/MEMS) devices using graphene sheets, the present results would be useful.

2 NONLOCAL PLATE MODEL

The nonlocal elasticity theory was introduced by Eringen (1983). In this theory, the stress state at a given point depends on the strain states at all points, while in the local theory, the stress state at any given point depends only on the strain state at that point. Stress components for a linear homogenous nonlocal elastic body without the body forces using nonlocal elasticity theory, we have (Eringen 1983):

$$\sigma_{ij}(x)=\int \lambda\left(\left|x-x'\right|,\gamma\right)C_{ijkl}\varepsilon_{kl}(x')dV(x'),\ \forall x\in V, \tag{1}$$

where σ_{ij}, ε_{ij} and C_{ijkl} are the stress, strain and fourth order elasticity tensors, respectively. The term $\lambda\left(\left|x-x'\right|,\gamma\right)$ is the nonlocal modulus (attenuation function) incorporating into constitutive equations the nonlocal effects. γ ($\gamma = e_0 l_i/a$) is a material constant that depends on the internal a (lattice parameter, granular size, distance between $C-C$ bonds), and external characteristics lengths l (crack length, wave length), l. Choice of the value of parameter e_0 is vital for the validity of nonlocal models. Hence the effects of small scale and atomic forces are considered as material parameters in the constitutive equation. This parameter was determined by matching the dispersion curves based on the atomic models. The term $\left|x-x'\right|$ represents the distance between the two points (x and x').The differential form of Eq. (1) can be written as (Malekzadeh et al 2011):

$$\left(1-\left(e_0 l_i\right)^2 \nabla^2\right)\sigma^{nl} = [C]\left[\{\varepsilon\}-\{\lambda\}\Delta T\right] \tag{2}$$

where σ^{nl}, ε, and λ denote the nonlocal stress, strain, and stress–temperature coefficients vectors, respectively. ΔT is the temperature change, C denote the elastic stiffness tensor. ∇^2 is the Laplacian operator that is defined by $\nabla^2 = (\partial^2/\partial x^2 + \partial^2/\partial y^2)$. The nonlocal constitutive equation Eq. (2) has been lately employed for the study of micro- and nano-structural elements. We consider nano monolayer orthotropic graphene sheets in our present study. In two-dimensional forms Eq. (2) are written as (Malekzadeh et al 2011):

$$\begin{Bmatrix}\sigma_{xx}^{nl}\\ \sigma_{yy}^{nl}\\ \sigma_{xy}^{nl}\end{Bmatrix} - (e_0 l_i)^2 \nabla^2 \begin{Bmatrix}\sigma_{xx}^{nl}\\ \sigma_{yy}^{nl}\\ \sigma_{xy}^{nl}\end{Bmatrix} = \begin{bmatrix} E_1/(1-\upsilon_{12}\upsilon_{21}) & \upsilon_{12}E_2/(1-\upsilon_{12}\upsilon_{21}) & 0 \\ \upsilon_{12}E_2/(1-\upsilon_{12}\upsilon_{21}) & E_2/(1-\upsilon_{12}\upsilon_{21}) & 0 \\ 0 & 0 & 2G_{12}\end{bmatrix}\begin{Bmatrix}\varepsilon_{xx}-\alpha_{xx}\Delta T\\ \varepsilon_{yy}-\alpha_{yy}\Delta T\\ \varepsilon_{xy}\end{Bmatrix} \tag{3}$$

where E_1 and E_2 are the Young's modulus, and G_{12} is shear modulus, υ_{12} and υ_{21} indicate Poisson's ratio , and α_{xx} and α_{yy} are the coefficient of thermal expansion along the principle material directions x and y, respectively. The strains in terms of displacement components in the middle surface can be written as follows (Malekzadeh et al 2011):

$$\varepsilon_{xx} = \frac{\partial u_0}{\partial x} - z\frac{\partial^2 w}{\partial x^2}, \quad \varepsilon_{yy} = \frac{\partial v_0}{\partial y} - z\frac{\partial^2 w}{\partial y^2}, \quad \varepsilon_{xx} = \frac{1}{2}\left(\left(\frac{\partial u_0}{\partial y} + \frac{\partial v_0}{\partial x}\right) - 2z\frac{\partial^2 w}{\partial x \partial y}\right) \tag{4}$$

In the foregoig, the first terms on the right-hand sides of the above equations represent the strain components in the middle surface due to its stretching, and terms with w represent the strain components due to bending. Stress resultants are defined as below for development of rectangular nanoplate (Pradhan and Phadikar 2009).

$$N_{xx} = \int_{-h/2}^{h/2} \sigma_{xx}^{nl} dz, N_{yy} = \int_{-h/2}^{h/2} \sigma_{yy}^{nl} dz, N_{xy} = \int_{-h/2}^{h/2} \sigma_{xy}^{nl} dz, M_{xx} = \int_{-h/2}^{h/2} z\sigma_{xx}^{nl} dz,$$
$$M_{yy} = \int_{-h/2}^{h/2} z\sigma_{yy}^{nl} dz, M_{xy} = \int_{-h/2}^{h/2} z\sigma_{xy}^{nl} dz \tag{5}$$

Here h is defined as the thickness of the plate. By inserting Eq. (3), and Eq. (4) into Eq. (5) we can express stress resultants in terms of lateral deflection on the classical plate theory as follows (Pradhan and Phadikar 2009):

$$M_{xx}-(e_0l_i)^2\nabla^2M_{xx}=-D_{11}\frac{\partial^2w}{\partial x^2}-D_{12}\frac{\partial^2w}{\partial y^2},M_{yy}-(e_0l_i)^2\nabla^2M_{yy}=-D_{12}\frac{\partial^2w}{\partial y^2}-D_{22}\frac{\partial^2w}{\partial x^2}$$
$$M_{xy}-(e_0l_i)^2\nabla^2M_{xy}=-2D_{66}\frac{\partial^2w}{\partial x\partial y}, \tag{6}$$

where D_{ij} indicate the different bending rigidity is defined as (Pradhan and Phadikar 2009):

$$\begin{Bmatrix}D_{11}\\D_{12}\\D_{22}\\D_{66}\end{Bmatrix}=\int_{-h/2}^{h/2}\begin{Bmatrix}E_1/(1-\upsilon_{12}\upsilon_{21})\\\upsilon_{12}E_2/(1-\upsilon_{12}\upsilon_{21})\\E_2/(1-\upsilon_{12}\upsilon_{21})\\G_{12}\end{Bmatrix}z^2dz \tag{7}$$

Note that stress resultants relations given in Eq. (6) reduce to that of the classical equation when the small scale coefficient (e_0l_i) is set to zero. A mono-layered rectangular graphene sheet embedded in an elastic medium (polymer matrix) is shown in Figure 1. A Pasternak-type foundation model is considered for simulating the elastic medium (polymer matrix) which accounts for both normal pressure and the transverse shear deformation of the surrounding elastic medium. The vibration equation for the orthotropic rectangular nanoplates is expressed as

$$\frac{\partial^2M_{xx}}{\partial x^2}+2\frac{\partial^2M_{xy}}{\partial x\partial y}+\frac{\partial^2M_{yy}}{\partial y^2}+f+\overline{N}_{xx}^T\frac{\partial^2w}{\partial x^2}+\overline{N}_{yy}^T\frac{\partial^2w}{\partial y^2}+2\overline{N}_{xy}^T\frac{\partial^2w}{\partial x\partial y}$$
$$-\overline{K}_WW+\overline{K}_{Gx}\frac{\partial^2w}{\partial x^2}+\overline{K}_{Gy}\frac{\partial^2w}{\partial y^2}=I_0\frac{\partial^2w}{\partial t^2}-I_2\left(\frac{\partial^4w}{\partial x^2\partial t^2}+\frac{\partial^4w}{\partial y^2\partial t^2}\right) \tag{8}$$

where $\overline{K}_W$ denote the Winkler modulus, $\overline{K}_{Gx}$ and $\overline{K}_{Gy}$ are the shear modulus of the surrounding elastic medium. If polymer matrix is homogeneous and isotropic, we will get $\overline{K}_{Gx}=\overline{K}_{Gy}=\overline{K}_G$. If the shear layer foundation stiffness is neglected, Pasternak foundation tends to Winkler foundation. The term f indicate transverse loading, I_0 and I_2 are mass moments of inertia that are defined as follows

$$I_0=\int_{-h/2}^{h/2}\rho dz,\quad \mathrm{I}_2=\int_{-h/2}^{h/2}\rho z^2dz \tag{9}$$

where ρ indicates the density of the graphene sheets. Also resultant thermal stresses $\overline{N}_{ij}^T$ (i, j=x, y) are defined as (Malekzadeh et al 2011):

$$\overline{N}_{xx}^{T} = -\left(E_1\alpha_{xx} / (1-\upsilon_{12}\upsilon_{21}) + \upsilon_{12}E_2\alpha_{yy} / (1-\upsilon_{12}\upsilon_{21})\right)h\Delta T$$
$$\overline{N}_{yy}^{T} = -\left(E_2\alpha_{yy} / (1-\upsilon_{12}\upsilon_{21}) + \upsilon_{12}E_2\alpha_{xx} / (1-\upsilon_{12}\upsilon_{21})\right)h\Delta T \quad (10\text{ a-c})$$
$$\overline{N}_{xy}^{T} = 0$$

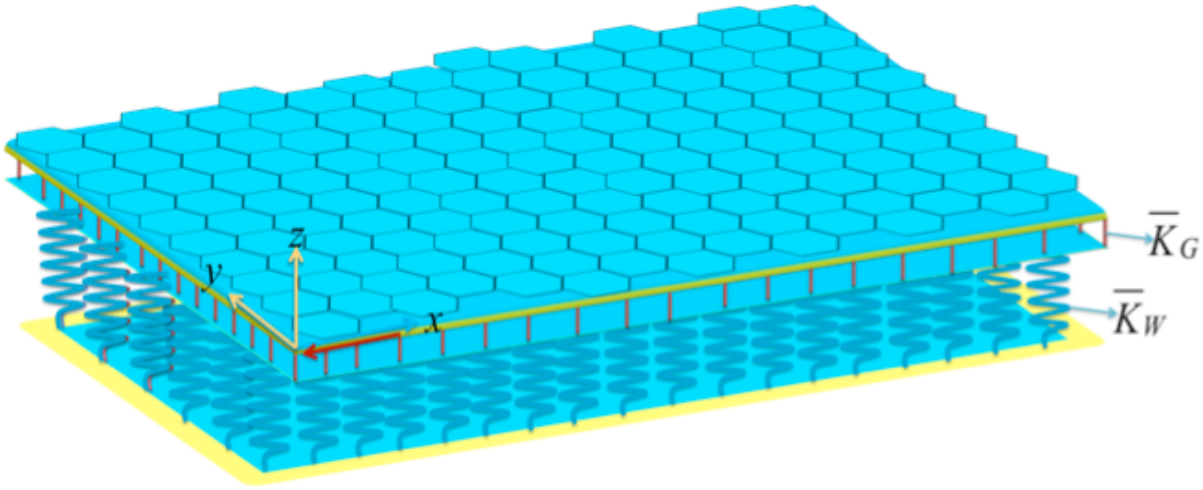

Figure 1 rectangular nanoplate embedded in an elastic medium

So we have Using Equations (6) and (8) we have the following governing equation in terms of the lateral deflection

$$D_{11}\frac{\partial^4 w}{\partial x^4} + 2\left(D_{12}+2D_{66}\right)\frac{\partial^4 w}{\partial x^2\partial y^2} + D_{22}\frac{\partial^4 w}{\partial y^4}$$
$$+\left(e_0 l_i\right)^2\nabla^2\begin{pmatrix} f + \overline{N}_{xx}^{T}\dfrac{\partial^2 w}{\partial x^2} + \overline{N}_{yy}^{T}\dfrac{\partial^2 w}{\partial y^2} - I_0\dfrac{\partial^2 w}{\partial t^2} + I_2\left(\dfrac{\partial^4 w}{\partial t^2\partial x^2} + \dfrac{\partial^4 w}{\partial t^2\partial y^2}\right) \\ -\overline{K}_W W + \overline{K}_{Gx}\dfrac{\partial^2 w}{\partial x^2} + \overline{K}_{Gy}\dfrac{\partial^2 w}{\partial y^2}\end{pmatrix} \quad (11)$$
$$-\begin{pmatrix} f + \overline{N}_{xx}^{T}\dfrac{\partial^2 w}{\partial x^2} + \overline{N}_{yy}^{T}\dfrac{\partial^2 w}{\partial y^2} - I_0\dfrac{\partial^2 w}{\partial t^2} + I_2\left(\dfrac{\partial^4 w}{\partial t^2\partial x^2} + \dfrac{\partial^4 w}{\partial t^2\partial y^2}\right) \\ -\overline{K}_W W + \overline{K}_{Gx}\dfrac{\partial^2 w}{\partial x^2} + \overline{K}_{Gy}\dfrac{\partial^2 w}{\partial y^2}\end{pmatrix} = 0.$$

At small scale, size effects can be noticeable in the mechanical properties of nanostructures. Both molecular dynamics simulation and experimental studies have shown that the size effect plays a prominent role in the static and dynamic characteristics of nanostructures. Chen et al.

(2004) investigated micro-continuum field theories such as couple stress theory, micromorphic theory, nonlocal theory, Cosserat theory from the atomistic viewpoint of lattice dynamics and molecular dynamics (MD) simulations. It is reported in their work that the nonlocal elasticity theory is physically reasonable.

3 SOLUTION PROCEDURES

It is assumed that the nanoplate is free from transverse loadings $(f=0)$. Exact solution of Equation (11) can be developed for some particular boundary conditions. In this article, initially, by using the Navier's approach orthotropic nanoplate problem is solved with simply supported boundary conditions. Then Levy type solution is used for orthotropic nanoplates, that at least for opposite edges, is simply supported.

3.1 Solution using Navier's approach

For simply supported boundary conditions, the shape function can be given by double Fourier series (Aksencer and Aydogdu, 2011)

$$w(x,y,t)=\sum_{m=1}^{\infty}\sum_{n=1}^{\infty}W_{mn}\sin(\frac{m\pi x}{a})\sin(\frac{n\pi y}{b})e^{i\omega t} \tag{12}$$

where m and n are the half wave numbers. Substituting from Equation (12) into Equation (11) yields the nondimensional natural frequency at small scale with various nanoplate properties, Winkler and shear elastic factors and resultant thermal stresses.

$$\begin{aligned}
&D_{11}(\frac{m\pi}{a})^4+2\left(D_{12}+2D_{66}\right)(\frac{m\pi}{a})^2(\frac{n\pi}{b})^2+D_{22}(\frac{n\pi}{b})^4\\
&+\left(e_0l_i\right)^2\overline{N}_{xx}^T\left((\frac{m\pi}{a})^4+(\frac{m\pi}{a})^2(\frac{n\pi}{b})^2\right)+\left(e_0l_i\right)^2\overline{N}_{yy}^T\left((\frac{n\pi}{b})^4+(\frac{m\pi}{a})^2(\frac{n\pi}{b})^2\right)\\
&+\left(e_0l_i\right)^2\overline{K}_W\left((\frac{m\pi}{a})^2+(\frac{n\pi}{b})^2\right)+\left(e_0l_i\right)^2\overline{K}_{Gx}\left((\frac{m\pi}{a})^4+(\frac{m\pi}{a})^2(\frac{n\pi}{b})^2\right)\\
&+\left(e_0l_i\right)^2\overline{K}_{Gy}\left((\frac{n\pi}{b})^4+(\frac{m\pi}{a})^2(\frac{n\pi}{b})^2\right)+\overline{N}_{xx}^T(\frac{m\pi}{a})^2+\overline{N}_{yy}^T(\frac{n\pi}{b})^2\\
&+\overline{K}_W+\overline{K}_{Gx}(\frac{m\pi}{a})^2+\overline{K}_{Gy}(\frac{n\pi}{b})^2-I_0\omega^2-I_2\omega^2\left((\frac{m\pi}{a})^2+(\frac{n\pi}{b})^2\right)\\
&-I_0\left(e_0l_i\right)^2\omega^2\left((\frac{m\pi}{a})^2+(\frac{n\pi}{b})^2\right)-I_2\left(e_0l_i\right)^2\left((\frac{m\pi}{a})^4+2(\frac{m\pi}{a})^2(\frac{n\pi}{b})^2+(\frac{n\pi}{b})^4\right)=0.
\end{aligned} \tag{13}$$

With multiply Equation (13) in a^4/D_{11} we have

$$\begin{aligned}
&\alpha^4+2\lambda_1\kappa^2\alpha^2\beta^2+\lambda_2\kappa^4\beta^4+K_{Gy}\left(\kappa^4\beta^2+\mu^2\left(\kappa^6\beta^4+\kappa^4\alpha^2\beta^2\right)\right)\\
&+K_{Gx}\left(\alpha^2+\mu^2\left(\alpha^4+\kappa^2\alpha^2\beta^2\right)\right)+N_{xx}^T\left(\alpha^2+\mu^2\left(\alpha^4+\kappa^2\alpha^2\beta^2\right)\right)\\
&+N_{yy}^T\left(\kappa^2\beta^2+\mu^2\left(\kappa^4\beta^4+\kappa^2\alpha^2\beta^2\right)\right)+K_W\left(\mu^2\left(\alpha^2+\kappa^2\beta^2\right)+1\right)\\
&-\mu^2\frac{I_0\omega^2a^4}{D_{11}}\left(\alpha^2+\kappa^2\beta^2\right)-\frac{I_0\omega^2a^4}{D_{11}}-\mu^2\frac{I_2\omega^2a^2}{D_{11}}\left(\alpha^4+2\kappa^2\beta^2\alpha^2+\kappa^4\beta^4\right)\\
&-\frac{I_2\omega^2a^2}{D_{11}}\left(\alpha^2+\kappa^2\beta^2\right)=0.
\end{aligned}\tag{14}$$

From Equation (9) we have

$$I_0=\rho h,\ I_2=\frac{\rho h^3}{12}\tag{15}$$

where nondimensional frequency parameter and other terms are defined in the following form

$$\begin{aligned}
&\Omega=\sqrt{\frac{\rho h}{D_{11}}}\omega a^2,\ \mu=\frac{e_0l_i}{a},\ \alpha=m\pi,\ \beta=\mathrm{n}\pi,\ \kappa=\frac{a}{b},\ \varepsilon=\frac{h}{\sqrt{12}a},\ \lambda_1=\frac{D_{12}+2D_{66}}{D_{11}},\\
&\lambda_2=\frac{D_{22}}{D_{11}},\mathrm{K}_W=\frac{\overline{K}_W a^4}{D_{11}},\ \mathrm{K}_{Gx}=\frac{\overline{K}_{Gx}a^2}{D_{11}},\ \mathrm{K}_{Gy}=\frac{\overline{K}_{Gy}b^2}{D_{11}},\ N_{xx}^T=\frac{\overline{N}_{xx}^T a^2}{D_{11}},\ N_{yy}^T=\frac{\overline{N}_{yy}^T a^2}{D_{11}}\\
&\bar{I}_0=\Omega^2=\frac{\rho h}{D_{11}}\omega^2a^4,\ \bar{I}_2=\Omega^2\varepsilon^2=\frac{\rho h^3}{12D_{11}}\omega^2a^2
\end{aligned}\tag{16}$$

With Substituting Equation (15) in Equation (14) we have

$$\begin{aligned}
&\alpha^4+2\lambda_1\kappa^2\alpha^2\beta^2+\lambda_2\kappa^4\beta^4+K_{Gy}\left(\kappa^4\beta^2+\mu^2\left(\kappa^6\beta^4+\kappa^4\alpha^2\beta^2\right)\right)\\
&+K_{Gx}\left(\alpha^2+\mu^2\left(\alpha^4+\kappa^2\alpha^2\beta^2\right)\right)+N_{xx}^T\left(\alpha^2+\mu^2\left(\alpha^4+\kappa^2\alpha^2\beta^2\right)\right)\\
&+N_{yy}^T\left(\kappa^2\beta^2+\mu^2\left(\kappa^4\beta^4+\kappa^2\alpha^2\beta^2\right)\right)+K_W\left(\mu^2\left(\alpha^2+\kappa^2\beta^2\right)+1\right)\\
&-\mu^2\frac{\rho h\omega^2a^4}{D_{11}}\left(\alpha^2+\kappa^2\beta^2\right)-\frac{\rho h\omega^2a^4}{D_{11}}-\mu^2\frac{\rho h^3\omega^2a^4}{12a^2D_{11}}\left(\alpha^4+2\kappa^2\beta^2\alpha^2+\kappa^4\beta^4\right)\\
&-\frac{\rho h^3\omega^2a^4}{12a^2D_{11}}\left(\alpha^2+\kappa^2\beta^2\right)=0.
\end{aligned}\tag{17}$$

Substituting $\bar{I}_0 = \Omega^2 = \left(\rho h / D_{11}\right)\omega^2 a^4$ and $\bar{I}_2 = \Omega^2 \varepsilon^2 = \left(\rho h^3 / 12 D_{11}\right)\omega^2 a^2$ in Equation (17) leads to

$$\begin{aligned}
&\alpha^4 + 2\lambda_1\kappa^2\alpha^2\beta^2 + \lambda_2\kappa^4\beta^4 + K_{Gy}\left(\kappa^4\beta^2 + \mu^2\left(\kappa^6\beta^4 + \kappa^4\alpha^2\beta^2\right)\right)\\
&+K_{Gx}\left(\alpha^2 + \mu^2\left(\alpha^4 + \kappa^2\alpha^2\beta^2\right)\right) + N_{xx}^T\left(\alpha^2 + \mu^2\left(\alpha^4 + \kappa^2\alpha^2\beta^2\right)\right)\\
&+N_{yy}^T\left(\kappa^2\beta^2 + \mu^2\left(\kappa^4\beta^4 + \kappa^2\alpha^2\beta^2\right)\right) + K_W\left(\mu^2\left(\alpha^2 + \kappa^2\beta^2\right) + 1\right)\\
&-\mu^2\bar{I}_0\left(\alpha^2 + \kappa^2\beta^2\right) - \bar{I}_0 - \mu^2\bar{I}_2\left(\alpha^4 + 2\kappa^2\beta^2\alpha^2 + \kappa^4\beta^4\right)\\
&-\bar{I}_2\left(\alpha^2 + \kappa^2\beta^2\right) = 0.
\end{aligned} \tag{18}$$

By arranging Equation (18) in term of Ω^2 leads to

$$\Omega^2 = \frac{\left(\begin{aligned}
&\alpha^4 + 2\lambda_1\kappa^2\alpha^2\beta^2 + \lambda_2\kappa^4\beta^4 + K_{Gy}\left(\kappa^4\beta^2 + \mu^2\left(\kappa^6\beta^4 + \kappa^4\alpha^2\beta^2\right)\right)\\
&+K_{Gx}\left(\alpha^2 + \mu^2\left(\alpha^4 + \kappa^2\alpha^2\beta^2\right)\right) + N_{xx}^T\left(\alpha^2 + \mu^2\left(\alpha^4 + \kappa^2\alpha^2\beta^2\right)\right)\\
&+N_{yy}^T\left(\kappa^2\beta^2 + \mu^2\left(\kappa^4\beta^4 + \kappa^2\alpha^2\beta^2\right)\right) + K_W\left(\mu^2\left(\alpha^2 + \kappa^2\beta^2\right) + 1\right)
\end{aligned}\right)}{\left(\alpha^2 + \kappa^2\beta^2\right)\left(\varepsilon^2 + \mu^2\left(\varepsilon^2\left(\alpha^2 + \kappa^2\beta^2\right) + 1\right)\right) + 1} \tag{19}$$

3.2 Solution using Levy type

To solve Equation (11) for a rectangular nanoplate with arbitrary boundary conditions, Levy's type of solution can be applied to nanoplates that are simply supported at two opposite edges. Assuming that the simple supports are at $x = 0$ and $x = a$, the shape function takes the form as (Aksencer and Aydogdu, 2011):

$$w(x,y,t) = X(x)Y(y)e^{i\omega t} = \sum_{m=1}^{\infty} Y(y)\sin\left(\frac{m\pi x}{a}\right)e^{i\omega t} \tag{20}$$

Substituting of Equation (20) into Equation (11) leads to

$$Y^{(4)} - 2BY^{(2)} + C = 0 \tag{21}$$

where B and C constants are the following form

$$B=\frac{\left(\begin{array}{l}2\lambda_1\kappa^2\alpha^2+K_{Gy}\left(\mu^2\kappa^4\alpha^2+\kappa^4\right)+K_W\mu^2\kappa^2+K_{Gx}\mu^2\kappa^2\alpha^2+N_{yy}^T\left(\mu^2\kappa^2\alpha^2+\kappa^2\right)\\+N_{xx}^T\mu^2\kappa^2\alpha^2-\Omega^2\left(\mu^2\kappa^2+2\mu^2\kappa^2\alpha^2\varepsilon^2+\kappa^2\varepsilon^2\right)\end{array}\right)}{2\left(\lambda_2\kappa^4+\mu^2K_{Gy}\kappa^6-\Omega^2\mu^2\varepsilon^2\kappa^4+N_{yy}^T\mu^2\kappa^4\right)} \tag{22}$$

$$C=\frac{\left(\begin{array}{l}K_W\left(\mu^2\alpha^2+1\right)+K_{Gx}\left(\mu^2\alpha^4+\alpha^2\right)+\alpha^4+N_{xx}^T\left(\mu^2\alpha^4+\alpha^2\right)\\-\Omega^2\left(\mu^2\alpha^2+\mu^2\alpha^4\varepsilon^2+\alpha^2\varepsilon^2+1\right)\end{array}\right)}{\left(\lambda_2\kappa^4+\mu^2K_{Gy}\kappa^6-\Omega^2\mu^2\varepsilon^2\kappa^4+N_{yy}^T\mu^2\kappa^4\right)} \tag{23}$$

Substituting $Y(y)=e^{sy}$ into Equation (21)

$$S^4-2BS^2+C=0 \tag{24}$$

Hence, for the orthotropic rectangular nanoplate, using the Levy-type solution requires four different forms of solution of $Y(y)$ to be put in Equation (20) depending on the relative rigidity of the nanoplate in various directions, Winkler elastic and shear elastic factor, nonlocal parameter and thermal change. the roots in the form as follows

For the case $0<C<B^2$

The general solution for $Y(y)$ is found to be

$$Y(y)=C_1\sinh(\delta_1 y)+C_2\cosh(\delta_1 y)+C_3\sinh(\delta_2 y)+C_4\cosh(\delta_2 y) \tag{25}$$

where

$$\delta_1=\sqrt{B+\sqrt{B^2-C}},\quad \delta_2=\sqrt{B-\sqrt{B^2-C}} \tag{26}$$

For the case $B^2=C$

$$Y(y)=(C_1^*+C_2^*y)\cosh(\delta_3 y)+(C_3^*+C_4^*y)\sinh(\delta_3 y) \tag{27}$$

where the roots are

$$\delta_3=\left(B\right)^{1/2} \tag{28}$$

For the case $C > B^2$

$$\begin{aligned} Y(y) = &(C_1^{**}\cos(\delta_5 y) + C_2^{**}\sin(\delta_5 y))\cosh(\delta_4 y) \\ &+ (C_3^{**}\cos(\delta_5 y) + C_4^{**}\sin(\delta_5 y))\sinh(\delta_4 y) \end{aligned} \tag{29}$$

where the roots are

$$\delta_4 = \left(\frac{1}{2}\left[\sqrt{C} + B\right]\right)^{1/2}, \quad \delta_5 = \left(\frac{1}{2}\left[\sqrt{C} - B\right]\right)^{1/2} \tag{30}$$

For the case $C < 0$

$$Y(y) = C_1^{***}\sin(\delta_6 y) + C_2^{***}\cos(\delta_6 y) + C_3^{***}\sinh(\delta_7 y) + C_4^{***}\cosh(\delta_7 y) \tag{31}$$

where the roots are

$$\delta_6 = \sqrt{\sqrt{B^2 - C} - B}, \quad \delta_7 = \sqrt{\sqrt{B^2 - C} + B} \tag{32}$$

Obviously, for a given nanoplate whose nonlaocal parameter, shear and Winkler elastic factors and other parameters have been specified only one of the four case needs to be solves to obtain frequency equations. The constants (C_i, C_j^*, C_k^{**},C_l^{***} (i,j,k,l=1,2,3,4)) are determined from the boundary conditions at $y = 0$ and $y = b$. The boundary conditions yield the frequency equation from which ω is determined. The procedure is shown below for three states boundary conditions and for case $C < 0$ the procedure for other cases is similar. The boundary conditions for simply supported edges, for instance, are

$$\mathrm{Y(0)=Y(b)=}\left.\frac{d^2Y}{dy^2}\right|_{y=0} = \left.\frac{d^2Y}{dy^2}\right|_{y=b} = 0 \tag{33}$$

Using Equation (31), the boundary conditions of Equation (33) can be expressed as

$$\begin{aligned} C_2^{***} + C_4^{***} &= 0 \\ \delta_6^2 C_2^{***} - \delta_7^2 C_4^{***} &= 0 \\ C_1^{***}\sin(\delta_6 b) + C_2^{***}\cos(\delta_6 b) + C_3^{***}\sinh(\delta_7 b) + C_4^{***}\cosh(\delta_7 b) &= 0 \\ C_1^{***}\delta_6^2\sin(\delta_6 b) + C_2^{***}\delta_6^2\cos(\delta_6 b) - C_3^{***}\delta_7^2\sinh(\delta_7 b) - C_4^{***}\delta_7^2\cosh(\delta_7 b) &= 0 \end{aligned} \tag{34-a-d}$$

Equations (34a, b) yield

$$C_2^{***} = C_4^{***} = 0 \tag{35}$$

Equations (34c, d) can be written in matrix form as

$$\begin{bmatrix} \sin(\delta_6 b) & \sinh(\delta_7 b) \\ -\delta_6^2 \sin(\delta_6 b) & \delta_7^2 \sinh(\delta_7 b) \end{bmatrix} \begin{Bmatrix} C_1^{***} \\ C_3^{***} \end{Bmatrix} = 0 \tag{36}$$

For a nontrivial solution, we should have $\sin(\delta_6 b) = 0$ or $\delta_6 = n\pi/b$. When edge $y = 0$ and $y = b$ are clamped. The boundary conditions can be stated as

$$\mathrm{Y(0)} = \mathrm{Y(b)} = \left.\frac{dY}{dy}\right|_{y=0} = \left.\frac{dY}{dy}\right|_{y=b} = 0 \tag{37}$$

By inserting Equation (31) into Equation (37), the boundary conditions can be written in matrix form as

$$\begin{bmatrix} 0 & 1 & 0 & 1 \\ \sin(\delta_6 b) & \cos(\delta_6 b) & \sinh(\delta_7 b) & \cosh(\delta_7 b) \\ \delta_6 & 0 & \delta_7 & 0 \\ -\delta_6 \cos(\delta_6 b) & \delta_6 \sin(\delta_6 b) & -\delta_7 \cosh(\delta_7 b) & -\delta_7 \sinh(\delta_7 b) \end{bmatrix} \begin{Bmatrix} C_1^{***} \\ C_2^{***} \\ C_3^{***} \\ C_4^{***} \end{Bmatrix} = 0 \tag{38}$$

By setting the determinant of the matrix in Equation (38) equal to zero, we obtain the frequency characteristic equation.

$$2\delta_6\delta_7\left(\cos(\delta_6 b)\cosh(\delta_7 b) - 1\right) - \left(\delta_7^2 - \delta_6^2\right)\sin(\delta_6 b)\sinh(\delta_7 b) = 0 \tag{39}$$

When the one edge of the rectangular nanoplate is clamped and other edge is simple supported, the additional four boundary conditions are

$$\mathrm{Y(0)} = \mathrm{Y(b)} = \left.\frac{d^2Y}{dy^2}\right|_{y=0} = \left.\frac{dY}{dy}\right|_{y=b} = 0 \tag{40}$$

Based on these boundary conditions, the coefficient determinant becomes

$$\begin{bmatrix} 0 & 1 & 0 & 1 \\ \sin(\delta_6 b) & \cos(\delta_6 b) & \sinh(\delta_7 b) & \cosh(\delta_7 b) \\ 0 & -\delta_6^2 & 0 & \delta_7^2 \\ -\delta_6 \cos(\delta_6 b) & \delta_6 \sin(\delta_6 b) & -\delta_7 \cosh(\delta_7 b) & -\delta_7 \sinh(\delta_7 b) \end{bmatrix} \begin{Bmatrix} C_1^{***} \\ C_2^{***} \\ C_3^{***} \\ C_4^{***} \end{Bmatrix} = 0 \tag{41}$$

A nontrivial solution can be obtained by equating the determinant of these equations to zero. Consequently, we have

$$\delta_7 \cosh(\delta_7 b)\sin(\delta_6 b) - \delta_6 \sinh(\delta_7 b)\cos(\delta_6 b) = 0 \tag{42}$$

For any specific value of m, there will be successive value of Ω. The natural frequencies can be denote as ω_{11}, ω_{12}, ω_{13}, ..., ω_{21}, ω_{22}, ..., whose value depend on the material properties E_1, E_2, υ_{12}, υ_{12}, ρ, α_{xx}, α_{yy} and geometry h, a/b and nonlocal parameter of the rectangular nanoplate. The frequency characteristic equations and the mode shapes for other case can be derived in a similar manner. The results for the three combinations of boundary conditions are summarized in Table 1. According to Table 1, by inserting $Y(y)$ into Equation (20) we have mode shape for orthotropic rectangular nanoplates based on elastic medium for different boundary conditions. Following three boundary conditions have been investigated in the vibration analysis of the rectangular graphene sheets as: SSSS, SCSC and SSSC that refer to Appendix 7.2 for more detail.

Table 1 Frequency equation and mode shape orthotropic rectangular nanoplates with different boundary conditions

Boundary conditions	**Type**	**Equation**
SSSS	Mode shape $Y(y)$	$\sin(\beta_n y) \qquad \beta_n = n\pi/b$
SCSC	Mode shape $Y(y)$	$\begin{Bmatrix} (\cosh(\delta_7 b)-\cos(\delta_6 b))(\delta_6 \sinh(\delta_7 y)-\delta_7 \sin(\delta_6 y)) \\ -(\delta_6 \sinh(\delta_7 b)-\delta_7 \sin(\delta_6 b))(\cosh(\delta_7 y)-\cos(\delta_6 y)) \end{Bmatrix}$
SSSC	Mode shape $Y(y)$	$\sin(\delta_6 b)\sinh(\delta_7 y)-\sinh(\delta_7 b)\sin(\delta_6 y)$

The mode shape of orthotropic rectangular nanoplate plays a significant role in the design of the nanomechanical resonators. It is observed that the single-layered graphene sheet with three cases of boundary conditions has a sinusoidal and/or hyperbolic sine and cosine configuration (Sakhaee-Pour et al 2006).

4 RESULTS AND DISCUSSION

4.1 Validation of present results

To validate the results, comparison of the present results for orthotropic rectangular nanoplate embedded in an elastic medium with the obtained results by DQM (Pradhan and Kumar 2010) is studied. In the present study non-dimensional frequency are calculated for all edges Simply Supported boundary conditions, these results are listed in Table 2.

Table 2 Comparison of results for vibration of the graphene sheet for all edges simply supported. (* (Pradhan and Kumar 2010)).

K_W	K_G	Method	$e_0 l_i$ (nm)				
			0	0.5	1	1.5	2
0	0	DQM*	19.3488	18.8885	17.6823	16.1011	14.4640
		Present	19.3489	18.8884	17.6822	16.1010	14.4638
	10	DQM*	23.9036	23.5328	22.5762	21.3604	20.1552
		Present	23.9039	23.4885	22.4139	21.0391	19.6644
400	0	DQM*	27.8145	27.4967	26.6837	25.6621	24.6678
		Present	27.8140	27.4957	26.6815	25.6609	24.6666
	10	DQM*	31.1554	30.8535	30.1995	29.3428	28.5086
		Present	31.1550	30.8375	30.0270	29.0153	28.0344

From this table one could find that the present results for the nanoplate exactly match with those reported by Pradhan and Kumar (2010). The scale coefficients are assumed as $e_0 l_i = 0.0,\ 0.5,\ 1.0,\ 1.5,$ and 2.0 nm, respectively. The value of nonlocal parameter is taken in the range of 0–2 nm. Duan and Wang (2007) presented the constitutive relations of nonlocal elasticity theory for application in the analysis of circular graphene sheet. Recently, these values for the nonlocal parameter are used by many researchers (Farajpour et al 2011b; Danesh et al. 2012; Farajpour et al 2012; Mohammadi et al. 2013b). Properties of the orthotropic graphene sheet in this paper are considered same as mentioned in the reference (Liew et al 2006).

$E_1 = 1765$ Gpa, $E_2 = 1588$ Gpa, $\upsilon_{12} = 0.3$, $\upsilon_{21} = 0.27$, $\rho = 2300\ kg/m^3$,

The material properties for isotropic graphene sheet are taken from Ref. (Liew et al 2006). $E_1, E_2 = 1060$ Gpa, $\rho = 2250\ kg/m^3$, $\upsilon_{12} = \upsilon_{21} = 0.25$.

The coefficients of thermal expansion are considered for orthotropic graphene sheet $\alpha_{yy} = \alpha_{xx}/3$ from Ref. (Malekzadeh et al 2011) and for isotropic graphene sheet are taken $\alpha_{xx} = \alpha_{yy}$. For the room or low temperature case thermal coefficient is taken $\alpha_{xx} = -1.6 \times 10^{(-6)}\ \mathrm{K}^{-1}$ and for high temperature case that is considered $\alpha_{xx} = 1.1 \times 10^{(-6)}\ \mathrm{K}^{-1}$. These values were used for carbon nanotube (Zhang et al. 2007).

The present results are compared to that obtained by Pradhan and Kumar (2011). Table 3 presents the non-dimensional frequency of orthotropic square nanoplate for two set boundary

condition. In this table, the Winkler factor and shear factor are ignored. These results are exactly in agreement with that presented by Pradhan and Kumar (2011).

Table 3 Comparison of results for vibration of the orthotropic graphene sheet for two set boundary conditions. (** (Pradhan and Kumar 2011)).

Method	$e_0 l_i$ (nm)				
	0	0.5	1	1.5	2
	SCSS boundary conditions				
DQM**	22.9849	22.4022	20.8867	18.9234	16.9171
Present	22.9849	22.4021	20.8865	18.9230	16.9166
	SCSC boundary conditions				
DQM**	27.9208	27.1853	25.2818	22.8350	20.3555
Present	27.9207	27.1851	25.2813	22.8341	20.3543

For further validations, we compared the results of rectangular nanoplates with published data. As shown in Table 4 results of Aksencer and Aydogdu (2011), compared to results obtained by present work for isotropic rectangular nanoplates without consider effect of elastic medium and thermal effect. These results are exactly in agreement with that presented by Aksencer and Aydogdu (2011).

Table 4 Comparison of results for vibration of the isotropic graphene sheet for three set boundary conditions.

	$e_0 l_i$ (nm)				
	0	0.5	1	1.5	2
	SSSS boundary conditions				
Aksencer and Aydodu (2011)	19.7205	19.2512	18.0218	16.4102	14.7415
Present	19.7205	19.2512	18.0218	16.4102	14.7415
	SCSS boundary conditions				
Aksencer and Aydodu (2011)	23.6223	23.0229	21.4641	19.4451	17.3823
Present	23.6223	23.0229	21.4641	19.4451	17.3823
	SCSC boundary conditions				
Aksencer and Aydodu (2011)	28.9203	28.1577	26.1844	23.6484	21.0791
Present	28.9203	28.1577	26.1844	23.6484	21.0791

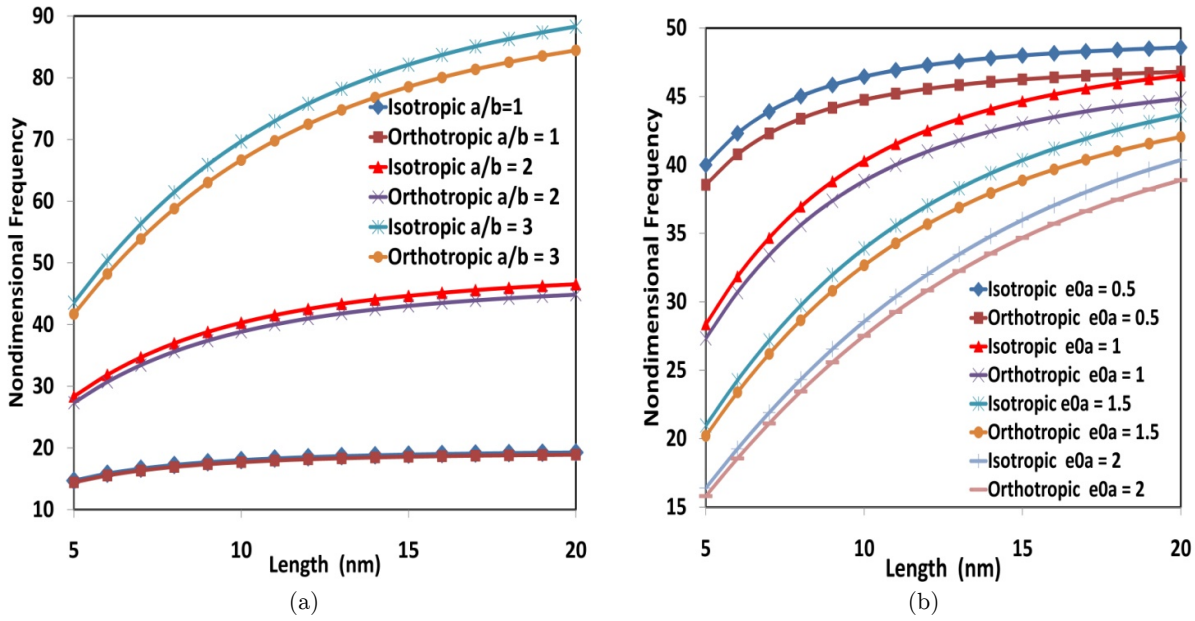

Figure 2 Change non-dimensional frequency with length of orthotropic and isotropic rectangular nanoplate for SSSS boundary condition and e_0l_i=1 nm (a) various aspect ratios (b) various nonlocal parameters (a/b=2).

4.2 Length effects on the frequency of orthotropic graphene sheet

Figures 2a, b shows the nondimensional natural frequency versus length of plate for isotropic and orthotropic graphene sheets and different aspect and nonlocal parameter. Figure 2a is plotted for SSSS case of boundary conditions, first mode and the nonlocal parameter 1 nm. This figure shows non-dimensional frequency versus length of for different aspect ratio and isotropic and orthotropic properties of graphene. As the length of the nanoplates decreases the non-dimensional frequency decreases. This is obvious because with decrease of length, the influence of nonlocal effect increase, at higher length all results converge to the local frequency. This indicates that the nonlocal effect disappears after a certain length and grows with decrease of the plate length. This may be explained as that the wavelength gets smaller with decrease of side length which increases the effect of the small length scale. Moreover, from this figure it is seen, that the non-dimensional frequency increases with the increase in aspect ratio, at higher aspect ratio all results converge to the local solution (e_0l_i=0) at higher lengths. This is evinced that effect of small length scale is higher for higher aspect ratio. Furthermore, the difference between the natural frequencies calculated by isotropic and orthotropic properties increases with increasing aspect ratio and length of nanoplate. This is shown that the difference between the natural frequencies calculated by isotropic and orthotropic for nonlocal solution is smaller as compared to local solution. Figure 2b shows the nondimensional natural frequency versus nonlocal parameter of isotropic and orthotropic graphene sheets without considering temperature change, first modeand SSSS boundary condition. In this figure aspect ratio is considered 2. This is shown that the difference between the natural frequencies calculated by isotropic and orthotropic for nonlocal solution is smaller as compression local solution. Also, it is observed that the nondimensional natural frequency increases with increasing length of nanoplates.

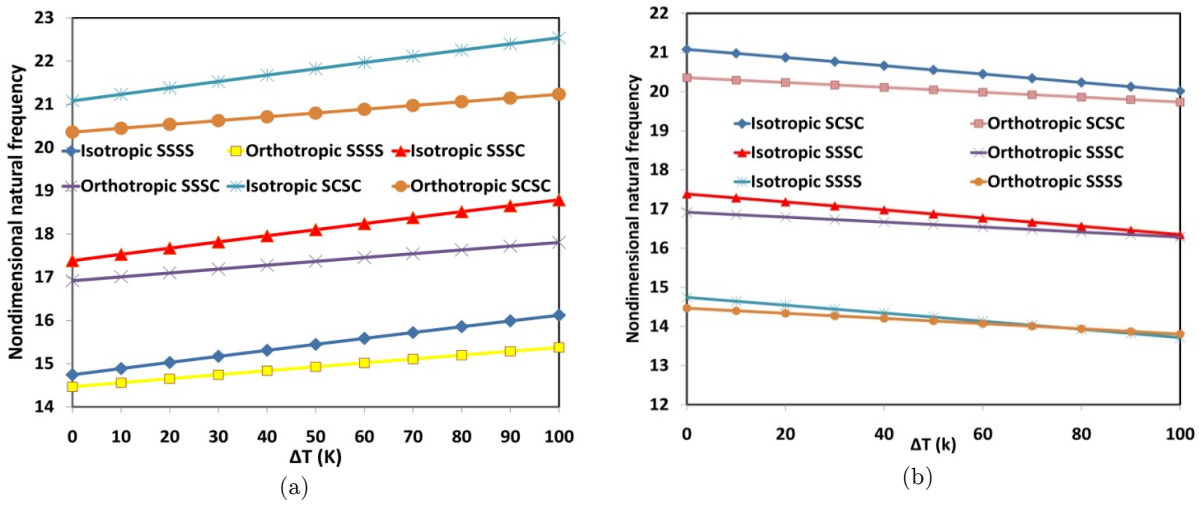

Figure 3 Change non-dimensional frequency with temperature change for various boundary conditions and isotropic and orthotropic graphene sheet in the case of (a) low temperature (b) high temperature. (a/b= 1, $e_o l_i$=2 nm)

4.3 Effects of temperature case on the frequency of orthotropic graphene sheet

To study the influence of low and high temperature case on the vibration characteristics of rectangular nanoplates, the variation in non-dimensional natural frequency with the temperature change is shown in Figure 3. The curves are plotted for isotropic and orthotropic properties, first mode numbers and three cases boundary condition. The length of the square nanoplate, the nonlocal parameter and aspect ratio are considered 10 nm, 2 nm and 1 respectively. It is shown non-dimensional frequency of the isotropic small-sized graphene sheet is always larger than that of orthotropic one for case of low temperature in Figure 3a. Furthermore, the gap between the two curves (isotropic and orthotropic) increases with an increase in temperature changes. In other words, the difference between the natural frequencies calculated by isotropic and orthotropic properties decreases with decreasing temperature change. Moreover, for this case the non-dimensional frequency increases with increase the temperature change. The temperature change is important for graphene sheet with isotropic properties because the slope of curve isotropic is more than orthotropic curves. Also, it is seen from this results that the nondimensional natural frequency for SCSC boundary condition is higher than that for SSSC and SSSS at low temperature case.

To illustrate the effect of high temperature case on the non-dimensional frequency, in this section, the non-dimensional frequency versus temperature change for isotropic and orthotropic properties of nanoplate is plotted in Figure 3b. In this investigation, we consider the non-dimensional frequency of first mode, the length of the square nanoplate 10 nm and the nonlocal parameter is 2 nm. It is seen for high temperature case the non-dimensional frequency increases with decrease temperature change. It means that the effects of the temperature change on the non-dimensional frequency are different for the case of low and high temperature. In the high temperature case, after a certain temperature change the non-dimensional frequency of orthotropic graphene sheet is more than the non-dimensional frequency of graphene sheet with iso-

tropic properties. The phenomenon could be attributed to the fact that the coefficient of thermal expansion in case of orthotropic graphene sheet in compared with the isotropic grapheme sheet are much less in the "Y" direction. Also, it is seen from this results the non-dimensional natural frequency for SCSC boundary condition is higher than the non-dimensional natural frequency for SSSC and SSSS boundary conditions at high temperature case.

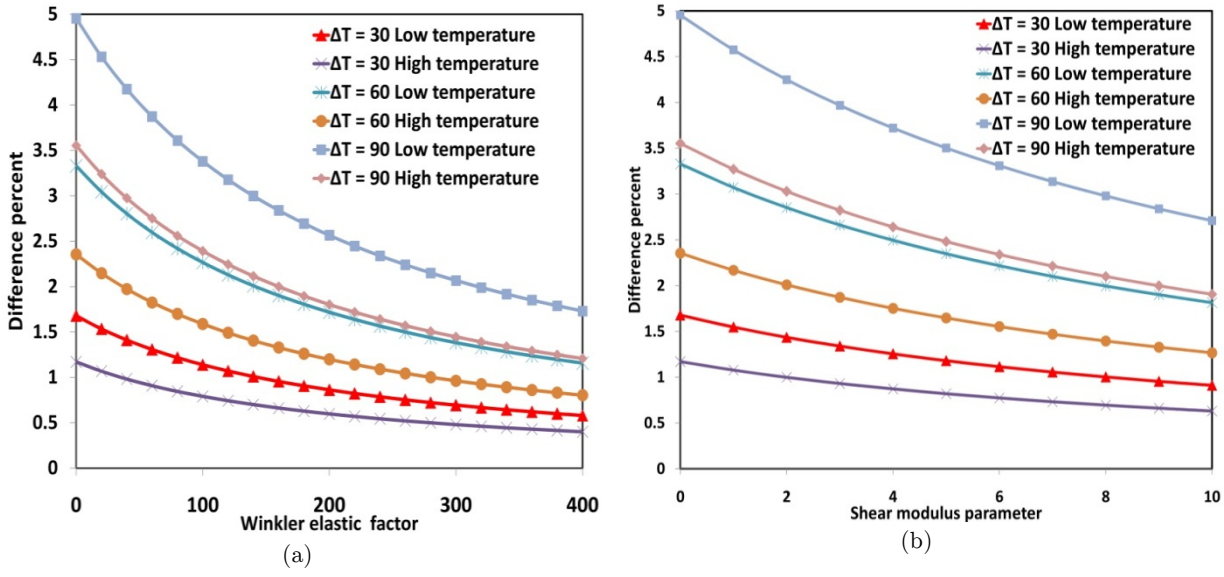

Figure 4 Variation of difference percent for various temperature changes of graphene sheet and low and high temperature case. (a) Shear modulus parameter (b) Winkler elastic factor. (SSSS boundary condition, a=10 nm, a/b=1, $e_o l_i$= 2 nm)

4.4 Elastic medium effects on natural frequency of orthotropic graphene sheet

The effect of temperature change on the frequency of orthotropic graphene sheet embedded in an elastic medium is studied. The Winkler modulus parameter K_W, for the surrounding polymer matrix is gotten in the range of 0–400. We assumed that polymer matrix is homogeneous $K_{Gx} = K_{Gy} = K_G$. Then shear modulus factor K_G is gotten in the range 0-10. Similar values of modulus parameter were taken by Liew et al. (2006). The relationships between frequency difference percent versus Winkler constant K_W and shear modulus K_G for different temperature changes and low and high temperature case are demonstrated in Figures 4a, b. A scale coefficient $e_0 a$ = 2.0 nm is used in the analysis. In this figure boundary condition, length of nanoplate and aspect ratio are assumed SSSS, 10 nm and 1 respectively. The frequency difference percent is defined as

$$\text{Difference percent} = \left| \frac{frequency_{\Delta T=T\ (K)} - frequency_{\Delta T=0}}{frequency_{\Delta T=0}} \right| \times 100$$

As can be seen, the Winkler constant or shear modulus decreases then the effect of thermal on the difference percent increases. It can be seen from the results that the difference percent increases with increasing the temperature change. For larger temperature change, the decline of difference percent is quite important. Also, the difference percent for low temperature case is larger than that for case of high temperature. Furthermore the decline for the high temperature case is much less than that for case of low temperature. From these plots obvious the important influence of temperature change, in the cases low and high temperature case on the non-dimensional frequency of embedded orthotropic graphene sheet.

4.5 Nonlocal effects on natural frequency of orthotropic graphene sheet

Figure 5 shows the frequency difference percent with respect to nonlocal parameter. In this investigation we consider SSSS boundary condition, a=10 nm and a/b=1. It is seen that the frequency difference percent increases with the increase of the temperature change. Also, the results show that the difference percent increases monotonically by increasing the nonlocal parameter. In other words, that nonlocal solution for difference percent is larger than the local solutions. In Figures 4a, b, and 5, the gap between low and high temperature cases increases with increasing the temperature change.

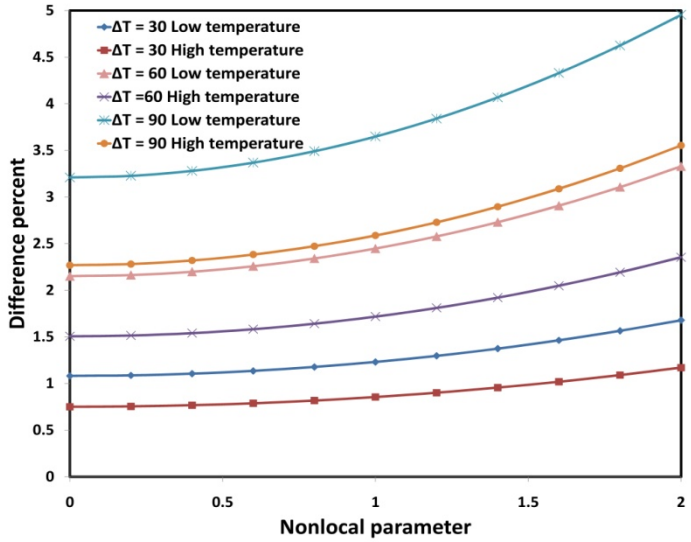

Figure 5 Variation of difference percent with nonlocal parameter for the cases low and high temperature and various changes temperature of orthotropic graphene sheet. (SSSS boundary condition, a=10 nm, a/b=1).

5 CONCLUSIONS

In this study, using the nonlocal elasticity continuum plate model, the effects of the temperature change on the vibration frequency of orthotropic and isotropic rectangular nanoplate embedded in an elastic medium was investigated for two cases low and high temperature. The elastic medium based on the Pasternak foundation was taken general case (the polymer matrix was considered non-homogeneous). Nonlocal elasticity theory has been applied to capture the structural discreteness of small-size plates (nanoplates). Equation of motion based on nonlocal theory has been derived. Exact closed form solutions for the free vibration nanoscale rectangular nanoplates are obtained using Navier's and Levy type solutions. Results for three set boundary condition are presented by levy type solution. From the results following conclusions are observed

- Small-scale effect has an increasing effect on the non-dimensional natural frequency of orthotropic and isotropic rectangular nanoplate. Scale effect is less prominent in lager length of nanoplate.
- The difference between the natural frequencies calculated by isotropic and orthotropic properties increases with increasing aspect ratio and length of nanoplate.
- The non-dimensional frequency is larger for higher aspect ratio and length of rectangular nanoplate.
- The non-dimensional natural frequency decreases at high temperature case with increasing the temperature change for all boundary conditions of isotropic and orthotropic rectangular graphene sheet.
- The effect of temperature change on the non-dimensional frequency vibration becomes the opposite at low temperature case in compression with the high temperature case.
- when Winkler or elastic factors increases, the frequency difference percent decreases at low and high temperature cases.
- The difference percent increases monotonically by increasing the nonlocal parameter.
- The difference between low and high temperature cases increases with increasing the temperature change.

References

Akgöz B., Civalek Ö. (2011a).Application of strain gradient elasticity theory for buckling analysis of protein microtubules. Current Applied Physics 11: 1133-1138.

Akgöz B., Civalek Ö. (2011b). Strain gradiant and modified couple stress models for buckling analysis of axially loaded micro-scales beam. International Journal of Engineering Science 49: 1268-1280.

Akgöz B., Civalek Ö. (2012a).Analysis of micro-sized beams for various boundary conditions based on the strain gradient elasticity theory. Archive of Applied Mechanics 82: 423-443.

Akgöz B., Civalek Ö. (2012b). Free vibration analysis for single-layered graphene sheets in an elastic matrix via modified couple stress theory. Materials & Design 42: 164-171.

Akgöz B., Civalek Ö. (2013a). A size-dependent shear deformation beam model based on the strain gradient elasticity theory. International Journal of Engineering Science 70: 1-14.

Akgöz B., Civalek Ö. (2013b). Modeling and analysis of micro-sized plates resting on elastic medium using the modified couple stress theory. Meccanica 48: 863-873.

Aksencer, T., Aydogdu, M. (2011). Levy type solution method for vibration and buckling of nanoplates using nonlocal elasticity theory. Physica E 43: 954 –959.

Babaei, H., Shahidi, A. R. (2010). Small-scale effects on the buckling of quadrilateral nanoplates based on nonlocal elasticity theory using the Galerkin method. Archive Applied Mechanics 81: 1051–1062.
Chen, Y., Lee, J.D., Eskandarian, A., (2004). Atomistic viewpoint of the applicability of microcontinuum theories. International Journal of Solids Structures 41: 2085-2097.
Civalek Ö., Akgöz B. (2013). Vibration analysis of micro-scaled sector shaped graphene surrounded by an elastic matrix. Computational Materials Science 77: 295-303.
Civalek Ö., Demir C., Akgöz B. (2010). Free Vibration and Bending Analyses of Cantilever Microtubules Based On Nonlocal Continuum Model. Mathematical and Computational Applications 15: 289-298.
Civalek Ö., Demir Ç. (2011).Bending analysis of microtubules using nonlocal Euler-Bernoulli beam theory. Applied Mathematical Modeling 35:2053-2067.
Demir Ç., Civalek Ö. (2013). Torsional and Longitudinal Frequency and Wave Response of Microtubules based on the Nonlocal Continuum and Nonlocal Discrete Models. Applied Mathematical Modeling http://dx.doi.org/10.1016/j.apm.2013.04.050067.
Duan, W.H., Wang, C.M. (2007). Exact solutions for axisymmetric bending of micro/nanoscale circular plates based on nonlocal plate theory. Nanotechnology 18: 385704.
Danesh, M., Farajpour, A., Mohammadi, M. (2012). Axial vibration analysis of a tapered nanorod based on nonlocal elasticity theory and differential quadrature method. Mechanics Research Communications 39: 23 –27.

Eringen, A.C. (1983). On differential equations of nonlocal elasticity and solutions of screw dislocation and surface waves. Journal Applied Physics 54: 4703-4711.
Farajpour, A., Mohammadi, M., Shahidi, A.R., Mahzoon, M. (2011a). Axisymmetric buckling of the circular graphene sheets with the nonlocal continuum plate model. Physica E 43: 1820 –1825.
Farajpour, A., Danesh, M., Mohammadi, M. (2011b). Buckling analysis of variable thickness nanoplates using nonlocal continuum mechanics. Physica E 44: 719 –727.
Farajpour, A., Shahidi, A.R., Mohammadi, M., Mahzoon, M. (2012). Buckling of orthotropic micro/nanoscale plates under linearly varying in-plane load via nonlocal continuum mechanics. Composite Structures 94: 1605 –1615.
Fleck, N. A., Hutchinson, J. W. (1997). Strain gradient plasticity. Applied Mechanics 33: 295–361.

Iijima, S. (1991). Helical microtubules of graphitic carbon. Nature 354: 56–58.

Kong, X.Y., Ding, Y., Yang, R., Wang, Z.L. (2004). Single-Crystal Nanorings Formed by Epitaxial Self-Coiling of Polar Nanobelts. *Science* 303: 1348-1351.

Liew, K. M., He, X. Q., Kitipornchai, S. (2006). Predicting nanovibration of multi-layered graphene sheets embedded in an elastic matrix. Acta Material 54: 4229-4236.
Malekzadeh, P., Setoodeh, A.R., Alibeygi Beni, A. (2011). Small scale effect on the thermal buckling of orthotropic arbitrary straight-sided quadrilateral nanoplates embedded in an elastic medium. Composite Structure 93: 2083–2089.
Mohammadi, M., Ghayour, M. Farajpour, A. (2013a). Free transverse vibration analysis of circular and annular graphene sheets with various boundary conditions using the nonlocal continuum plate model. Composites: Part B 45: 32–42.
Mohammadi, M., Goodarzi, M., Ghayour, M., Farajpour, A. (2013b). Influence of in-plane pre-load on the vibration frequency of circular graphene sheet via nonlocal continuum theory. Composites: Part B 51: 121–129.
Moosavi, H., Mohammadi, M., Farajpour, A., Shahidi, S.H. (2011). Vibration analysis of nanorings using nonlocal continuum mechanics and shear deformable ring theory. Physica E 44: 135 –140.
Murmu, T., Pradhan, S. C. (2009). Vibration analysis of nano-single-layered graphene sheets embedded in elastic medium based on nonlocal elasticity theory. Journal Applied Physic 105: 064319.
Pradhan, S. C., Kumar, A. (2010). Vibration analysis of orthotropic graphene sheets embedded in Pasternak elastic medium using nonlocal elasticity theory and differential quadrature method. Computational Material Science 50: 239-245.

Pradhan, S. C., Kumar, A. (2011). Vibration analysis of orthotropic graphene sheets using nonlocal theory and differential quadrature method. Compos Structure 93: 774-779.

Pradhan, S.C., Phadikar, J. K. (2009). Small scale effect on vibration of embedded multi layered graphene sheets based on nonlocal continuum models. Physics Letters A 373: 1062–1069.

Reddy, C. D., Rajendran, S., Liew, K.M. (2006). Equilibrium configuration and continuum elastic properties of finite sized grapheme. Nanotechnology 17: 864–870.

Sakhaee-Pour, A., Ahmadian, M. T., Naghdabadi, R. (2008). Vibrational analysis of single layered graphene sheets. Nanotechnology 19: 957–964.

Satish, N., Narendar, S., Gopalakrishnan, S. (2012). Thermal vibration analysis of orthotropic nanoplates based on nonlocal continuum mechanics. Physica E 44: 1950 –1962.

Sorop, T.G., Jongh, L. J. (2007). Size-dependent anisotropic diamagnetic screening in superconducting nanowires. Physic Review B 75: 014510.

Wang, Y. Z., Li, F. M., Kishimoto, K. (2011). Thermal effects on vibration properties of doublelayered nanoplates at small scales. Composites Part B: Engineering 42: 1311–1317.

Wong, E.W., Sheehan, P.E., Lieber, C.M. (1997). Nanobeam mechanics: elasticity, strength and toughness of nanorods and nanotubes. Science 277: 1971–1975.

Yang, F., Chong, A.C.M., Lam, D.C.C., Tong, P. (2002). Couple stress based strain gradient theory for elasticity. International Journal of Solids Structure 39: 2731-2743.

Zhang, Y.Q., Liu, X., Liu, G.R. (2007). Thermal effect on transverse vibrations of double walled carbon nanotubes. Nanotechnology 18: 445701.

Zhou, S.J., Li, Z.Q. (2001). Metabolic response of Platynota stultana pupae during and after extended exposure to elevated CO_2 and reduced O_2 atmospheres. Shandong University Technology 31: 401-409.